3 RANGE INCREASE OF ADAPTIVE AND PHASED ARRAYS IN THE PRESENCE OF INTERFERERS

3.1 Introduction

A higher directive gain at the base station will result in an increased signal level at the mobile receiver, allowing longer range operation or increased coverage. This increased range in a non-multipath environment is described in [45] for narrowband adaptive arrays and in [56] for a CDMA adaptive array. A comparison of the range increase of phased and adaptive arrays in a multipath environment for both narrow-band and spread-spectrum systems is given in [16].

In a phased array the signals received at the individual elements of the array are multiplied by a weight vector and then combined to form a beam in the direction of the desired mobile. The gain of the array (and associated range) will increase and beamwidth will decrease as the number of antenna elements at the base station is increased. The above statement will be valid until the beamwidth becomes comparable with the angular spread of the multipath signals. A further increase in the number of antenna elements will not necessarily result in a significant range increase, due to the loss in power from the scattering signal components arriving outside the array beamwidth. An adaptive array on the other hand optimizes the array pattern to maximize the array signal to interference plus noise ration (SINR) for the desired mobile. The result is that the adaptive array does not present the range limitation found in phased arrays.

In a wideband system, a RAKE receiver can be used to exploit the temporal characteristics of the propagation signal. The signal is combined coherently in time to give an increase in the signal strength through temporal diversity. By forming a different beam for each RAKE finger based on optimal signal to noise ratio, the range limitation of phased arrays can be reduced.

The purpose of this chapter is to present results of a comparative study of the range increase of adaptive versus phased arrays in a multipath environment. This study is an extension of the work presented in [16], with the effect of the presence of interference included in the present study. One of the major advantages of an adaptive array is the

ability to suppress interference, and one would expect the inclusion of the interference in the study would have a significant effect on the results. An approximation for the angle of arrival probability density function (PDF) for the circular vector channel model is also presented. A theoretical model using this PDF, which approximates the range increase of phased arrays in a multipath environment, is proposed.

The focus of this thesis is the performance of spatially distributed adaptive arrays in cellular networks. In TDMA systems, the spatially distributed array consists of sub-arrays located at alternate corners of a typical hexagonal cell structure. As a result of this geometry, the range between the arrays and mobiles can be larger than that of a conventional cell geometry, where the arrays (or sectorized antennas) are located at the center of the cell. Adaptive arrays offer a range increase relative to sectorized and phased arrays. However, this range increase is a function of the number and location of interferers as well as the propagation environment. This range increase is important to the distributed array operation. Although not directly applied to the spatially distributed array performance investigation in the rest of the thesis, it forms an important contribution to the overall spatially distributed array study. In addition, the results can be valuable to future studies on phased arrays applied to spatially distributed arrays systems.

The phased array range increase without multipath is presented in section 3.2. The array geometry and multipath model will be described in section 3.3, and the desired signal, interference and noise power at the output of the phased and adaptive arrays will be given. This is followed by the simulation procedure and simulation results for the narrow-band and spread-spectrum systems in section 3.4. An analytical model is derived for the range increase of phased arrays in a multipath environment in section 3.5, followed by conclusions in section 3.6.

3.2   Phased Array Range Increase without Multipath

In this section the range increase of a phased array relative to an omni (reference) antenna due to the increased gain of the array is described [16,32]. The power received at the omni antenna is:

$$P_{R,Omni} = \frac{P_T\, G_T\, G_R\, \lambda^2}{\left(4\pi r_0\right)^2 \left(\frac{r_{omni}}{r_0}\right)^\gamma} \tag{64}$$

where P_T is the mobile transmit power, G_R is the omni antenna gain, G_T is the mobile antenna gain, λ is the carrier wavelength, r_{omni}^γ is the range between the mobile and the omni antenna and γ is the power pathloss exponent and r_0 is the close in free space reference distance. The gain of an M-element array antenna is [16]:

$$G_{R,array} = M\, G_R \tag{65}$$

Inserting (65) in (64), the received signal of the array is:

$$P_{R,array} = \frac{M\, P_T\, G_T\, G_R\, \lambda^2}{\left(4\pi r_0\right)^2 \left(\frac{r_{array}}{r_0}\right)^\gamma} \tag{66}$$

The objective is now to calculate the range of the array relative to the range of the reference antenna for equal received signal strengths. This can be determined by setting (64) equal to (66):

$$\frac{P_T\, G_T\, G_R\, \lambda^2}{\left(4\pi r_0\right)^2 \left(\frac{r_{omni}}{r_0}\right)^\gamma} = \frac{M\, P_T\, G_T\, G_R\, \lambda^2}{\left(4\pi r_0\right)^2 \left(\frac{r_{array}}{r_0}\right)^\gamma} \tag{67}$$

or

$$\left(\frac{r_{array}}{r_{omni}}\right)^\gamma = M \tag{68}$$

Thus the range increase of an array relative to the reference (omni) antenna is:

$$\text{Range Increase} = r_{array} = M^{1/\gamma}\, r_{omni} \tag{69}$$

3.3   Array Geometry and Multipath Model

A circular array with M elements is used with cardoid element pattern as shown in Figure 9. The multipath geometry is shown in Figure 11 and Figure 12. The difference between

the mean angle of arrival of the desired and d^{th} multipath component is β_d^c, with $d \in \{1,2,...,D\}$ and D the total number of signals. The circular vector channel model is used [11,45], consisting of K scatterers uniformly distributed in a circular area with radius r_{max}^s around the desired and interfering signals. Assuming equal power scattered by the K objects, the baseband signal arriving at antenna element m from signal d is:

$$z_{m,d}(nT_s) = S_d(nT_s) X_{m,d}(nT_s) \tag{70}$$

where $S_d(t)$ is the baseband signal transmitted by mobile d. Using equation (24), the received signals at the antenna elements are:

$$X_{m,d}(nT_s) = \frac{1}{4\pi r_0} \sum_{k=1}^{K} \{ \frac{F(m,\psi_{d,k})}{\sqrt{K\left(\frac{r_{d,k}^e}{r_0}\right)^\gamma}} \delta(nT_s - \tau_{d,k})$$

$$\tag{71}$$

$$e^{j\left[(2\pi/\lambda)\left\{r_{d,k}^s + r_{d,k}^e\right\} + [\pi\Delta/\lambda \sin(\pi/M)]\cos\left\{\psi_{d,k} - 2\pi(m-1)/M\right\}\right]}\} + n_s(nT_s)$$

where λ is the carrier wavelength, Δ is the spacing between elements, T_s is the sample period, n is the sample number, $\tau_{d,k}$ is the delay between source d and array center via scatterer k, $r_{d,k}^s$ is the distance between the source d and scatterer k, $r_{d,k}^e$ is the distance between the scatterer k and the center of the circular array, γ is the pathloss exponent, $n_s(m,nT_s)$ is zero mean Gaussian noise at element m and $F(m,\psi_{d,k})$ is the mth element voltage pattern in direction $\psi_{d,k}$, given by:

$$F(m,\psi_{d,k}) = \sqrt{2}\cos\left[\frac{\pi}{4}\left(\cos\left\{\psi_{d,k} - \frac{2\pi(m-1)}{M}\right\} - 1\right)\right] \tag{72}$$

The phased and adaptive array desired signal, sum of interference and noise power at the output for narrow-band and spread-spectrum systems will be presented next.

3.3.1   Narrow-band Systems

The signal to interference plus noise ratio (SINR) can be written as [45]:

$$\text{SINR} = \frac{P_d \mathbf{W}^H \left\{ \mathbf{X}_1 \, \mathbf{X}_1^H \right\} \mathbf{W}}{\mathbf{W}^H \mathbf{R}_{nn} \mathbf{W} + \sigma_N^2 \mathbf{W}^H \mathbf{W}} \tag{73}$$

where $\mathbf{W}$ is the array beamforming weight vector, P_d is the desired signal power at the antenna elements, $\mathbf{X}_1^H$ is the complex conjugate transpose of the desired signal receive vector at the antenna elements given in (71), σ_N^2 is the noise power and $\mathbf{R}_{nn}$ is the interference plus noise covariance matrix. Assuming the signals are uncorrelated, $\mathbf{R}_{nn}$ is given by (see Appendix A):

$$\mathbf{R}_{nn} = \sum_{d=2}^{D} P_d \, \mathbf{X}_d \, \mathbf{X}_d^H + \sigma_N^2 \mathbf{I} \tag{74}$$

where $\mathbf{I}$ is the identity matrix, $\mathbf{X}_d^H$ is the complex conjugate transpose of the receive vector from the dth interferer receive vector at the antenna elements given in (71) and P_d is the power of the dth interferer. The weight vector $\mathbf{W}$ for the adaptive array is [54]:

$$\mathbf{W} = \mathbf{R}_{nn}^{-1} \mathbf{U}_1 \tag{75}$$

where $\mathbf{U}_1$ is the desired signal array vector. The phased array is steered towards the desired signal, with weight vector $\mathbf{w}$ given by [16]:

$$\mathbf{W} = \mathbf{U}_1 (\psi_1^c) \tag{76}$$

where $\mathbf{U}_1 (\psi_1^c)$ is the array vector of the desired signal in the direction of ψ_1^c.

3.3.2   Spread Spectrum Systems

In a wideband spread spectrum system, a RAKE receiver can be used to exploit the temporal characteristics of the propagation signal [16]. The signal strength is increased through temporal diversity by coherently combining the multipath signals in time. A three finger ($L = 3$) RAKE receiver (see section 2.6.2) on each antenna element is assumed in the simulations to follow. The spread spectrum processing (employing a RAKE receiver) is described next. Each source transmits a data sequence that is spreaded by a unique code. The multipath signals received from all the sources at each antenna element $\sum_{d=1}^{D} z_{m,d}(nT_s)$ was first correlated with the spreading code of the desired signal. The signals were then

weighed and summed. The three strongest peaks (or called fingers in CDMA) of the summed signal separated by integer multiples of the of the code rate were then detected with its corresponding time of arrival $n_\ell T_s$, where n_ℓ is the sample number of finger $\ell \in \{1,2,3\}$. The three fingers were then coherently added to yield the following desired array output power P^{des}:

$$P^{des} = P_d \; g_p \sum_{\ell}^{L} \left\{ \left| \sum_{m=1}^{M} W^*(m,\ell) \; v_1(m,n_\ell T_s) \right|^2 \right\} \tag{77}$$

where $v(m,n_\ell T_s)$ is the output signal of correlator m at time sample $n_\ell T_s$, $W^*(m,\ell)$ is the conjugate of complex weight m of finger ℓ and g_p is the processing gain. The processing gain is the same for the reference and array systems and will therefore be ignored in the comparison between systems. The interference power at the array output at time t_ℓ is:

$$P^{int} = \left| \sum_{\ell=1}^{L} \sum_{m=1}^{M} \left\{ W^*(m,\ell) \sum_{d=2}^{D} X_{m,d}(n_\ell T_s) \right\} \right|^2 \tag{78}$$

where $x_{m,d}(n_\ell T_s)$ is the baseband m^{th} element array signal of source d at time sample $n_\ell T_s$, given in (71). The weight vector $\mathbf{W}$ of the adaptive array for finger ℓ is:

$$\mathbf{W}(\ell) = \mathbf{R}_{nn,\ell}^{-1} \; \mathbf{U}_1(n_\ell T_s) \tag{79}$$

and for the phased array:

$$\mathbf{W}(\ell) = \mathbf{U}_1(\psi_1^c) \tag{80}$$

where $\mathbf{U}_1(n_\ell T_s)$ is the desired signal propagation vector in the direction of the multipath component at time sample $n_\ell T_s$, $\mathbf{U}_1(\psi_1^c)$ is the steering vector in the direction ψ_1^c of the desired signal and $\mathbf{R}_{nn,\ell}$ is the interference plus noise covariance matrix at time sample $n_\ell T_s$, given by (see Appendix A):

$$\mathbf{R}_{nn,\ell} = \sum_{d=2}^{D} \left\{ P_d \, \mathbf{X}_d(n_\ell T_s) \mathbf{X}_d^H(n_\ell T_s) \right\} + \sigma_N^2 \mathbf{I} \tag{81}$$

An alternative beamforming model alleviating the range limitation of the phased array was proposed in [2]. In this model a RAKE receiver is implemented before weighting and summing of the array signals. The RAKE receiver determines the three multipath fingers, followed by determination of an optimum array pointing direction for each finger. This is done by scanning (or changing the weight vector in (80)) the pointing direction ψ to either side of ψ_1^c for each finger and determining the array pointing direction which gives the maximum output power. This method is applied in the spread spectrum simulations to follow.

3.4   Comparative Study

The procedure that was followed here is similar to the procedure presented in [2]. The average bit error rate (BER) for coherent detection of phase-shift keying signals in a digital system is given in (63). With a specific scattering radius and range between the signal and the reference (omni-antenna) system, the transmitted signal to noise (SNR) and interference to noise ratio (INR) were adjusted until an average BER of 10^{-2} was obtained at the output of the reference system. Using this SNR and INR while the scattering radius is fixed, the range of the array was increased until an average BER of 10^{-2} was achieved. This array range relative to that of the reference system is now the range increase (or extension).

Monte-Carlo simulations (see section 2.9.1) were performed to determine the average BER. The pathloss coefficient γ for the range between each scatterer and the receiver was 4 ($\gamma = 4$) and a total of 20 scatterers were assumed. The effect of shadowing loss (see section 2.4.2) was not taken into account and the spacing between the antenna array elements was a half wavelength.

Narrowband and wideband (spread spectrum) systems with RAKE receivers were considered, as will be discussed next.

3.4.1   Narrow-band Systems

The range extension of adaptive and phased arrays for 10°, 20° and 45° angular spreads with a 16.7dB equal average SNR and SIR are shown in Figure 23, Figure 24 and Figure 25 respectively. Results are shown for both noise only (where the SNR was 13.7dB) and

one interferer cases, with the interferer located at various azimuth angles ψ^c relative to the boresight of the array. A single dominant interferer is typical in TDMA type cellular systems [59]. In order to obtain the same BER for noise only scenario and the scenario with a single interferer, the noise power was decreased when the interferer was added, such that the total SINR is equal to the SNR for the noise only case.
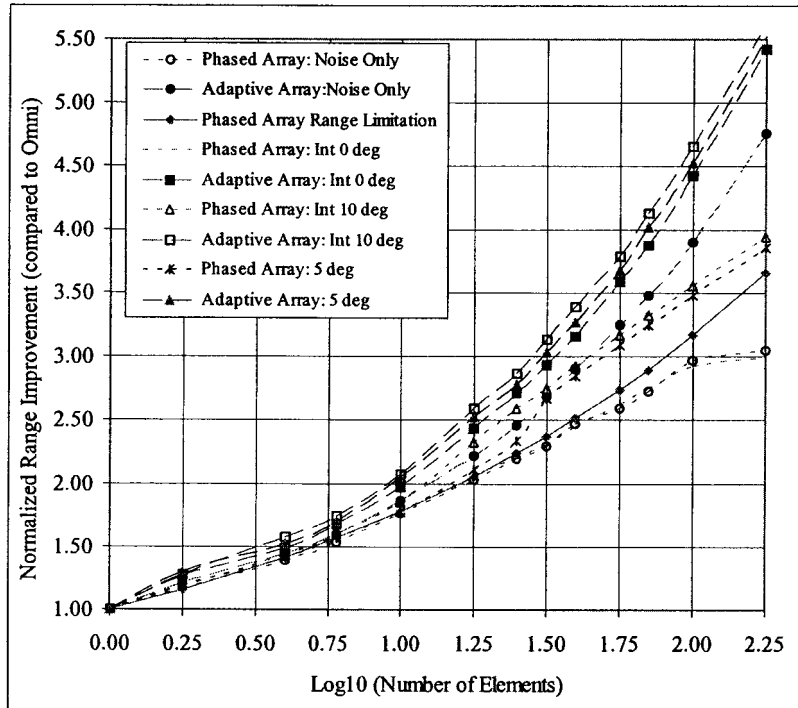

Figure 23: Adaptive and phased array range increase in a narrow-band system for a 10° angular spread, one interferer separated from the user by 0°, 5° and 10°.

**Figure 24 Adaptive and phased array range increase in a narrow-band system for a 20°
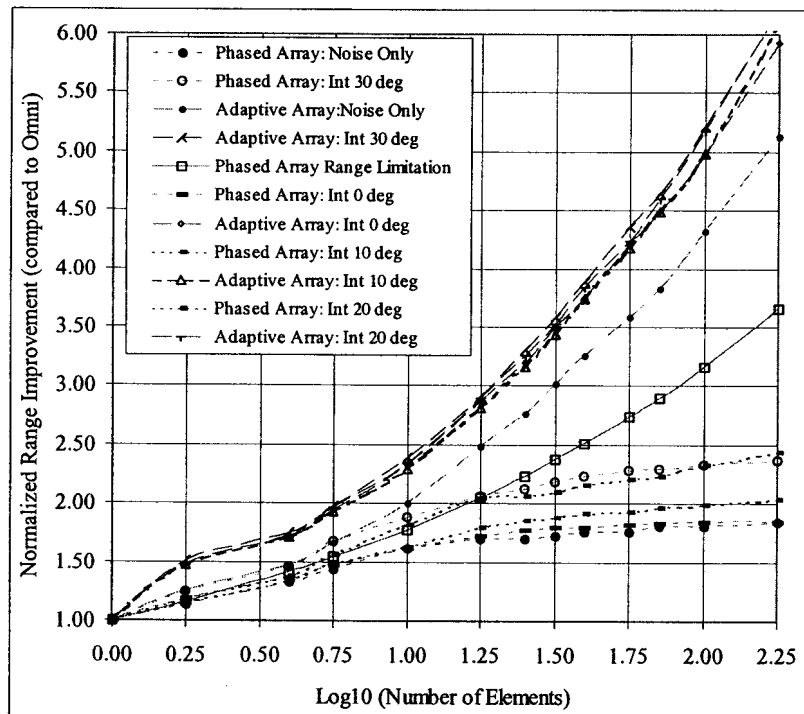angular spread, one interferer separated from the user by 0°, 5°, 10° and 20°.**

**Figure 25: Adaptive vs. phased array range increase in a narrow-band system for a 45°
angular spread, one interferer separated from the user by 0°, 10°, 20° and 30°.**

In Figure 23 with 10° angular spread, the phased array range extension with an interferer at 0° is the same as the noise only scenario. This is to be expected since the SINR (with an interferer) and SNR (without an interferer) was chosen to be equal, the phased array is not able to distinguish between the desired user and the interferer is contributing to the total system noise. The range increase of the 5° and 10° interferer cases is equal to the phased array noise only range limitation up to the point (approximately 1.5 for 5° case and 1.125 for 10° case) where the interferer angle starts to fall outside the beamwidth of the array. The phased array noise only range limitation is the range at which the array beamwidth becomes smaller than the multipath scattering angle (or angular spread), in which case the array increased gain is offset by the loss of energy falling outside the array beamwidth. When the interferer angle starts to fall outside the array beam, the array is able to cancel a part of the interfering signal, with the result that the range increase exceeds the noise only range increase.

Since the adaptive arrays are able to reduce the interfering signal multipath components (even when the interferer is in the same direction as the desired signal [45]) and constructively add the desired signal multipath components, it can be seen that the range increase exceeds the noise only adaptive array range increase.

3.4.2   Spread Spectrum Systems

In the spread spectrum simulations, it is assumed that there are 12 equal power interferers, randomly located in azimuth angle ψ_q^c. Twelve interferers are assumed, since this is typical for current tri-cellular CDMA systems [56]. The multipath model used for the spread spectrum simulations is similar to the narrowband model. Two signal to noise ratio (SNR) scenarios are investigated. The first is a SNR of 14dB, which comprises 7.5dB required receive energy per bit relative to the noise density Eb/No [12,56] and 6.5dB fading margin. In the second scenario a SNR of 11dB is assumed.

The range increase of adaptive vs. phased arrays for angular spreads of 20° and 45° is shown in Figure 26 and Figure 27 respectively. The phased array weight vector (or beam direction) is optimized for each delay.
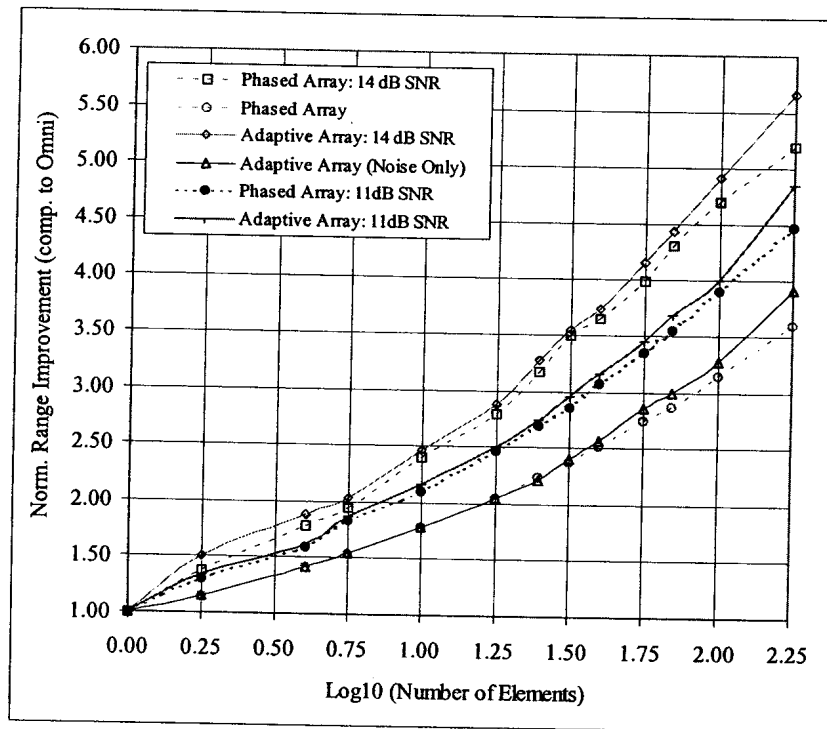
Figure 26: Adaptive vs. phased array range increase for a spread spectrum system with 20° angular spread, twelve randomly positioned interferers for 19.6dB, 11dB and 14dB signal to noise ratio.
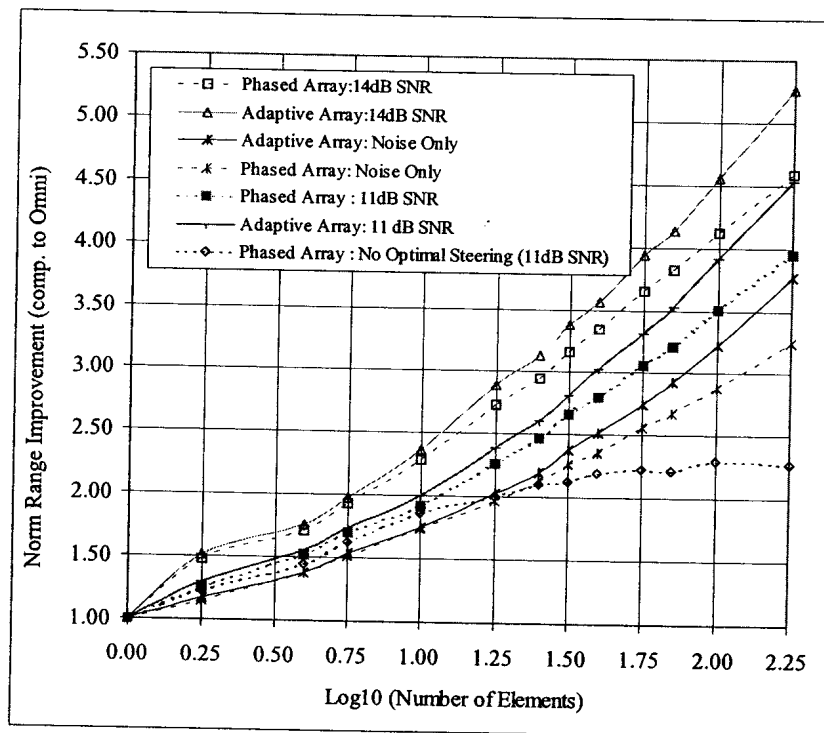

Figure 27 Adaptive vs. phased array range increase for a spread spectrum system with 45° angular spread, twelve randomly positioned interferers for 18.9dB, 11dB and 14dB signal to noise ratio.

In Figure 27 the non-optimized (beam pointing in fixed direction towards desired signal) phased array range increase is also shown. Note that apart from the 6.8dB RAKE diversity gain [16], the same range limitations as in the narrowband case is observed. This phased array range limitation is reduced by optimizing the weight vector for each delay. Since the adaptive array is able reduce the interfering multipath signals and coherently add the desired multipath signals (even if they fall inside the Fresnel beamwidth of the adaptive array), a larger range increase for the adaptive array relative to the phased array is observed (the phased array is unable to cancel interferer multipath signals that falls inside the array Fresnel beamwidth).

3.5   Analytical Model

In this section an analytical model is derived to predict the range improvement of a narrowband phased array in a multipath environment, including the presence of a single interferer. The typical angle of arrival histogram (PDF) of the multipath signal for the circular vector channel model [45] is shown in Figure 28 for an angular spread 40° ($\psi_{max} = 20°$). The probability of a signal arriving from an angle ψ can be approximated by:

$$P_{AOA}(\psi) = B \cos\left(\frac{\pi \psi}{\psi_{max}}\right)^{0.45} \tag{82}$$

where B is an arbitrary constant, which cancels in (84). This approximation is shown in Figure 28, with B = 1270 and $\psi_{max} = 20°$. It can be seen that the approximation is a good match to the histogram.
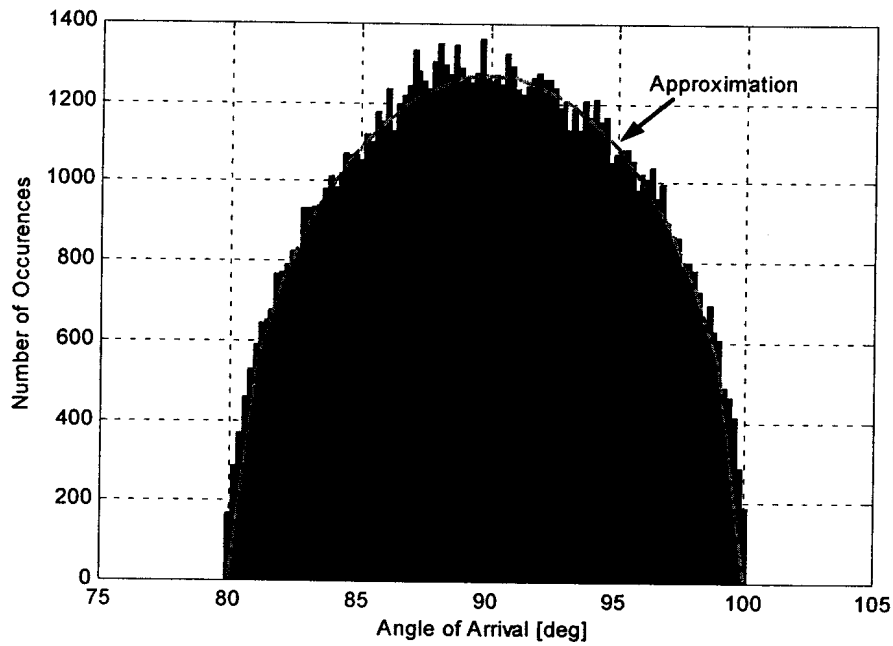
Figure 28: Angle of arrival histogram and approximation.

It was shown in the previous section that the range increase of a phased array in the presence of an interferer is reduced when the angular spread of the desired signal multipath components is wider than the beamwidth of the array. The multipath incident components will be weighted by the beam taper of the phased array. Components falling outside the 10dB beamwidth of the beam will contribute very little energy towards the total energy received by the array. However, the probability of signals arriving at these large angles is also lower as indicated by the PDF in Figure 28. Taking all these factors into account the SINR of a phased array can be approximated by the following equation:

$$SINR_{approx} = \frac{P_d \, M \, (1 - \aleph) / r_{incr}^{\gamma}}{(P_q \, M \, (1 - \aleph) / r_{incr}^{\gamma}) + \sigma_N^2} \qquad (83)$$

where P_d and P_q are the average power per element received from the desired and interference signals, respectively. These average powers are calculated for the omni antenna at a specific range as described earlier. r_{incr} is the ratio of the array to omni range, that is the range increase. This ratio is increased to the point where the SINR of the array equals that of the omni antenna. $\aleph$ is the power loss of the multipath components due to the antenna array azimuth pattern taper, r is the range between the center of the array and the mobiles, σ_N^2 is the noise power and γ is the pathloss exponent. The power loss is the

ratio of the maximum of the convolution of the array power pattern and the angle of arrival PDF to the total area of the angle of arrival PDF, given by:

$$\aleph = \frac{\displaystyle\int_{-\infty}^{\infty} P_{AOA}(\psi)\,G(\psi-\xi)\,d\xi}{\displaystyle\int_{-\psi_{max}}^{\psi_{max}} P_{AOA}(\psi)\,d\psi} \tag{84}$$

where $G(\psi)$ is the antenna array power pattern at angle ψ and P_{AOA} is the PDF of the angle of arrival. To find the range increase of the phased array relative to an omni, the distance between the desired user and the array is increased until the $SINR_{approx}$ matches the SINR for the onmi.

A comparison between the range increase possible for a phased array obtained through simulation (similar to section 3) and the analytical model derived (see equation (83)) is shown in Figure 29 for 10°, 20° and 45° angular spreads.
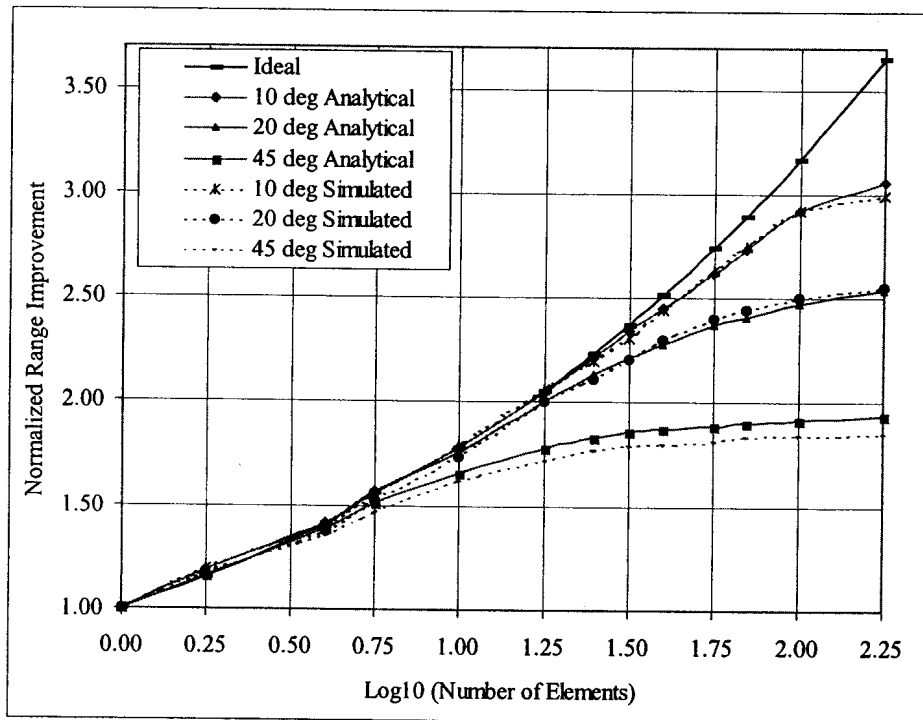

Figure 29: Comparison of simulated and analytical phased array range improvement for 10°, 20° and 45° angular spreads.

Using the approximate equations (82), (83) and (84) presented in this section, it is possible to estimate the range increase of a phased array in a multipath environment in the presence

of interferers using the analytical model derived instead of running time consuming simulations as was done in section 3.4. The results obtained with the analytical model gave accurate approximations for the results obtained through the Monte-Carlo simulations.

3.6   Conclusions

This chapter presented the effect of interference on the range increase (relative to an omni-antenna) of adaptive vs. phased arrays in a multipath environment for both narrowband and spread-spectrum systems.

The range increase of a narrowband cellular system with a single dominant interferer (typical for TDMA cellular systems) at various incidence angles was presented as a function of the number of array elements and scattering angular spread. The adaptive array is able to increase its range by reducing the contributions from the multipath components of the interferer, even when the interferer is in the same direction as the desired signal in low angular spread environment (10 degree angular spread). A phased array on the other hand, achieves a significant range increase when the beamwidth of the array becomes narrow enough that the multipath components of the interferer falls outside the beam of the array.

The range increase of wideband spread spectrums with twelve interferers per sector (typical for CDMA cellular systems) was presented as a function of the number of array elements, scattering angular spread and received signal to noise ratio. Similar to the results in [16], the range increase limitation of phased arrays in the presence of multiple interferers can be improved by using a weight vector optimized for each RAKE receiver finger. The results also showed that the range increase of phased arrays is less than that of adaptive arrays due to the lack of cancellation of interferer multipath components falling inside the beamwidth of the phased array.

An analytical model was derived to predict the range increase of a phased array in a multipath environment in the presence of a dominant interferer. The probability density function of the angle of arrival PDF of a circular vector channel model was approximated and then used in the analytical model to estimated the range increase possible with phased arrays. An asymptotic limit of the range increase possible with a phased array exists when

the array beamwidth becomes narrower than the desired signal angular spread. This limit is a function of the angular spread of the multipath.